

Valence bands of the Mg_2X ($X = Si, Ge, Sn$) semiconducting compounds

Javier Tejada and Manuel Cardona

Max-Planck-Institut für Festkörperforschung, Stuttgart, Federal Republic of Germany

(Received 23 February 1976)

Energy distribution spectra of photoelectrons excited by monochromatized Al $K\alpha$ radiation (XPS) from the valence bands of the Mg_2X semiconductors are presented. The results are compared with calculated densities of valence states obtained from parametrized tight-binding bands. The nearest-neighbor interaction parameters are determined so as to obtain theoretical total densities of valence states which fit the experimental XPS spectra and partial densities of states which agree with soft-x-ray emission data. The upper, p -like valence bands so determined agree well with the empirical pseudopotential calculations of Au-Yang and Cohen while discrepancies appear for the lower s bands. The parameters of the tight-binding model are compared with those reported recently by several authors for the elemental semiconductors.

I. INTRODUCTION

The semiconducting compounds¹⁻³ Mg_2X ($X=Si, Ge, Sn$) crystallize in the fcc antifluorite structure with one molecular unit per primitive cell. The remaining member of the family, Mg_2Pb , seems to be semimetallic.⁴ The low electric conductivity of these materials was interpreted by Mott and Jones⁵ on the basis of their band structure. Their 32 valence electrons per cubic unit cell (eight per primitive cell) suffice to fill completely the fourth Brillouin zone. The materials are actually isoelectronic to the germaniumlike semiconductors, and since they have the same translation lattice their band structures are very similar. Thus they may have a gap between occupied and unoccupied states, its existence and width being determined by the nature of the constituent atoms. As usual in families of semiconductors composed of atoms of the same column of the periodic table, the thermal gap decreases along the sequence $Mg_2Si-Mg_2Ge-Mg_2Sn-Mg_2Pb$.

Considerable information is available about the lattice dynamics of the Mg_2X materials. At $k=0$ there are two sets of optical phonons: those of Γ_{15} symmetry, infrared allowed and split into LO-TO, and those of $\Gamma_{25'}$ symmetry, Raman active. Detailed dispersion relations have been determined through neutron scattering only for Mg_2Sn .⁶ Nevertheless preliminary dispersion relations have also been obtained for⁷ Mg_2Si and⁸ Mg_2Ge by inter- and extrapolating the elastic constants, the infrared frequencies (Γ_{15} phonons at $k=0$) and the Raman frequencies. The second-order Raman spectra have yielded some information about phonons off $k=0$ while recent resonant Raman measurements have yielded considerable information about band structure and electron-phonon interaction.⁹

The relatively strong reststrahlen reflectivity

peaks¹⁰ point out to the ionic character of the bonding. On the basis of the Mg- X separation, the ionic, metallic and covalent radii, and the electronegativity of the constituents, Eldridge *et al.*¹¹ concluded that the bonding of the Mg_2X compounds is mostly covalent with only 10% ionic character. We believe this work strongly underestimates the ionic character of these compounds.

Electron density distribution measurements on Mg_2Si by Ageev and Guseva¹² indicate an almost spherical electron cloud around the Si and a highly distorted one around the Mg. Approximating these distributions by spheres, one accounts for 10 of the 12 electrons of Mg and all 14 of the Si electrons. From the charge density, it appears that one of the two missing electrons of Mg is involved in the Si-Si bond, and the other is shared between the Si and Mg in the Si-Mg bond. While one may be tempted to conclude from these facts that the Mg ions have a charge of +1.5 and the X ions a charge of -3, Ageev and Guseva refuse to give an estimate of ionicity of Mg_2Si . They argue that the absence of a sharp boundary between ions makes this estimate questionable. Recently, Panke and Woelfel¹³ obtained more accurate results for the electron density in Mg_2Si . They found that the charge distribution around the Mg has cubic shape while that around the Si is highly distorted. They estimate that 10.5 of the Mg electrons are situated in its surrounding cloud (corresponding indeed to a $Mg^{1.5+}$ ion). However, two of the eight valence electrons are distributed in the empty spaces between the ions. The values they find for the radii of the Mg and Si ions in Mg_2Si (1.00 and 1.75 Å, respectively) lie between the corresponding covalent and ionic radii.¹¹

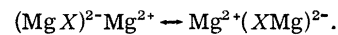
The band structure of the Mg_2X compounds has been the object of several experimental¹⁴⁻¹⁶ and theoretical¹⁷⁻²¹ studies. As usual in the field of semiconductors most of the theoretical treatments

use experimental parameters as input data to adjust the crystal potential. Maybe the most important of these parameters is the lowest (thermal) gap, found to be indirect and to equal 0.73 eV for Mg_2Si , 0.72 eV for Mg_2Ge , and 0.31 eV for Mg_2Sn .²⁰ The top of the valence band is at Γ (like in the germanium-type semiconductors) while the lowest conduction band-minimum seems to be at X (like in Si) for the three compounds under consideration.²² The spin-orbit splitting at the top of the valence band (Γ_{15}) has been measured to be for Mg_2Ge $\Delta_0 = 0.2$ eV, $\approx \frac{2}{3}$ of that found in elemental crystalline Ge (0.3 eV). A spin-orbit splitting of 0.2 eV is also found for the $4p$ levels of atomic Ge: the increase in the spin-orbit splitting when bringing the atoms together to form crystalline Ge is due to the corresponding compression of the $4p$ wave functions. This compression should barely take place in Mg_2Ge because of the larger Ge-Ge separation (4.52 Å) as compared with that in the elemental crystal (2.44 Å). Hence, the top of the valence band should be composed, in a linear combination of atomic orbitals (LCAO) picture, nearly exclusively of $4p$ wave functions of Ge. Likewise, $5p$ and $3p$ atomic functions of Sn and Si, respectively, are almost certain to form the top of the valence bands of Mg_2Sn and Mg_2Si .

We have recently published electron energy distribution spectra for the Mg_2X materials obtained with unmonochromatized²⁴ Al $K\alpha$ excitation [x-ray photoemission spectra (XPS)] (referred in this work as I) and with several uv lines between²⁵ 20 and 48 eV (referred as II). These spectra contain information about core levels and their chemical shifts and about the density of valence states. Information about the density of valence states was also obtained in I from the KLV Auger spectrum of the Mg constituent. This information suffers from a number of handicaps: The Auger density of states is heavily affected by energy-dependent matrix elements, the ultraviolet photoemission spectra are highly sensitive to surface contamination (II), and the work with unmonochromatized Al $K\alpha$ x-rays suffers from poor resolution (1.5 eV) and low signal-to-noise ratio. In the present work we report XPS measurements with monochromatized Al $K\alpha$ radiation for Mg_2Si , Mg_2Ge , and Mg_2Sn . Except for some well understood energy dependence of the matrix elements in Mg_2Si , the results obtained seem to yield, after correction for secondary electrons, a good picture of the total density of valence states (DOVS).

In order to interpret the measured DOVS we have performed theoretical DOVS calculations. It has been shown²⁶⁻³³ that the size of the secular matrices required to represent the valence bands of cubic semiconductors and insulators can be re-

duced considerably if an empirical tight-binding or molecular-orbital bonding approach is used. We used such an approach in our work. In anti-fluorite Mg_2X each Mg is surrounded by four X atoms situated at the corners of a tetrahedron while each X atom is the center of a cube containing eight Mg atoms at its corners. Since it is impossible to construct a set of eight orthogonal covalent bonds along the diagonals of the cube by using the $2s$ wave functions of Mg and the s and p valence electrons of X , a resonant model was proposed to interpret the bonding in Mg_2X .³³ According to this model half of the Mg atoms are at a given time covalently bonded to the X atoms in a tetrahedral configuration. These bonds resonate with the other possible tetrahedral configuration in which the remaining four Mg atoms participate. This model can be represented by the resonance of the configurations:



It is difficult to treat this model within the framework of a self-consistent-field band-structure picture with the full symmetry of the O_h cubic point group. In view of the strongly ionic nature of these materials pointed out above we have chosen for our band-structure calculations a completely ionic tight-binding model in which all of the valence electrons of Mg have been transferred to the X atom. The valence bands are thus composed of the s and p valence atomic orbitals of the X atom. The measured DOVS and the s partial densities of states, obtained from soft-x-ray emission spectra (SXS) for Mg_2Si , are used to determine the tight-binding parameters of our model. Detailed comparisons of our calculated valence bands with those obtained with the empirical pseudopotential methods by Au-Yang and Cohen²⁰ are given.

II. BAND-STRUCTURE CALCULATIONS

The first band-structure calculation for Mg_2X materials was performed by Della Riccia in 1960.¹⁷ Using a nearly-empty-lattice model, where the atomic potentials are included only to remove the accidental degeneracies. Della Riccia obtained a band structure equally applicable to all materials with anti-fluorite structure. These bands are quantitatively wrong: they correspond to metals and not to semiconductors. However the shapes of the conduction and valence bands considered separately are rather similar to those obtained later and confirmed by the experiments.

In 1964 Lee published calculations for Mg_2Si and Mg_2Ge using the pseudopotential method.¹⁸ This was probably the first time that the band structure of a compound was calculated with pseudopotential

coefficients not treated as adjustable parameters but obtained from the pure elements. Unfortunately the pseudopotentials for Mg were known only for $|k| < 2k_F$ (k_F is the Fermi momentum) and an extrapolation for higher values had to be used. These band structures, even though qualitatively correct, yield up to 1 eV higher energies for the optical interband transitions.

Folland¹⁹ calculated in 1967 the band structure of Mg_2Si using the Hartree self-consistent-field method. The results of these "first principles" calculations are quite different from those of other calculations and do not agree with the optical measurements reported later. Folland also performed calculations with the Hartree-Fock method but since they also are not in agreement with experiment these results were not reported in detail.

Au-Yang and Cohen (AC) used the empirical pseudopotential method (EPM) to calculate the band structure (see, for example, Fig. 1, dashed lines, and Sec. IV) and the $\epsilon_2(\omega)$ spectra of the Mg_2X compounds. They adjusted the pseudopotential form factors of the pure elements so as to obtain the experimental ϵ_2 spectra. The band gaps calculated in this work reproduce well those obtained from reflectivity¹⁵ and electroreflectance¹⁶ measurements. The position of the critical points in the calculated ϵ_2 spectrum, as well as their strength, is very similar to that obtained from the Kramers-Kronig analysis of reflectivity measurements. The main structures in the ϵ_2 spectra can be traced to pairs of valence and conduction bands that remain parallel over an extended portion of the Brillouin zone. AC's calculated ϵ_2 values are larger than the experimental ones at high energies, a discrepancy probably due to either an over-

estimate of the matrix elements (actually pseudo-matrix elements are employed), the locality of the pseudopotential used, or internal field corrections.

Folland and Bassani³⁴ discussed the symmetry selection rules for interband optical transitions in the antifluorite lattice and, from an analysis of mobility data, concluded that the minimum of the conduction band should be at the X point and have X_3 symmetry in Mg_2Si and Mg_2Sn . They cannot draw a conclusion from the data for Mg_2Ge . These minima in AC calculations are X_1 for Mg_2Si and Mg_2Sn , and X_3 for Mg_2Ge . This cannot be considered to be a major failure since in Mg_2Si and Mg_2Ge X_1 and X_3 are nearly degenerate (less than 0.2 eV difference) and only in Mg_2Sn are they clearly separated (0.6 eV).

Aymerich and Mula reported a new pseudopotential calculation in 1970.²¹ The only difference with that of AC is that they screened the pseudopotential form factors of Mg with the k -dependent dielectric constant of the compound (a semiconductor) instead of that of the pure metal. Their band structures are practically identical with those of AC, the only important difference is the symmetry of the conduction-band minimum: X_3 for Mg_2Si and Mg_2Sn , X_1 for Mg_2Ge (AC's are the opposite). These symmetries are in agreement with Folland and Bassani's analysis. Unfortunately Aymerich and Mula do not calculate the ϵ_2 spectra. They rely on the similarity of their bands to those of AC and expect ϵ_2 to be nearly the same. It would have been interesting to see if their bands give for ϵ_2 better agreement with experiment especially for Mg_2Sn , for which AC's calculations gives a less satisfactory fit.

Unfortunately, in spite of the large number of calculated band structures the corresponding densities of states were not obtained. We shall present in Sec. IV calculations of the density of valence states (DOVS) for Mg_2Si , Mg_2Ge , and Mg_2Sn .

III. EXPERIMENT

The measurements were performed in an HP 5950 A ESCA spectrometer with monochromatized Al $K\alpha$ radiation (1487.6 eV). The samples were sputtered in the preparation chamber onto a substrate at room temperature and transferred into the measuring chamber without breaking the vacuum. It has been shown in I and II that samples sputtered on substrates at room temperature are polycrystalline. (Other details are similar to those given in I and II.) The electron count rates for the spectra of the valence bands were small and required long measuring times, typically 8 h, to obtain satisfactory statistics. Since the samples

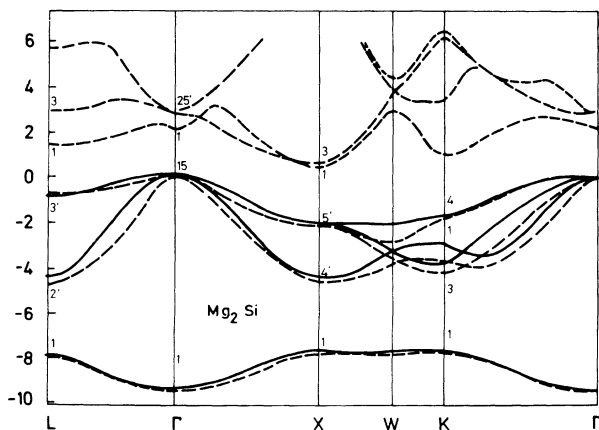


FIG. 1. Band structure of Mg_2Si calculated by Au-Yang and Cohen with the empirical pseudopotential method (EPM, dashed line) and fit to the EPM valence bands obtained with the ETBM (solid line). The energy is given in eV.

oxidize easily (see I and II) in spite of the good vacuum in the measuring chamber (better than 10^{-9} Torr), the oxygen contamination was checked periodically; it was found from the strength of the $1s$ XPS line that the oxygen absorbed in 2 h was about 1–2 monolayers. The escape depth at the energies of the Al $K\alpha$ radiation is about 10 monolayers (II) and thus the valence-band spectra of the oxidized material 2 h after sputtering should be nearly the same as those of the pure material. This is in sharp contrast with measurements for uv excitation in the conventional 20–40-eV range. At these photon energies a fraction of a monolayer obliterates the “clean” spectrum because of the small escape depth and the large emission efficiency of the oxide. After checking the oxygen absorption every 2 h, the films were resputtered so as to keep a sufficiently clean surface.

The photoelectron energy distribution spectra measured for the valence bands of Mg_2X are presented in Fig. 2. They are compatible with those previously obtained with unmonochromatized x rays (I) but they reflect the fact that resolution of the present measurement (0.6 eV) is about twice the one for the work with the unmonochromatized source (1.5 eV). The contribution from secondary electrons was estimated with the approximation that a δ function of primary electrons is followed by a step function of secondary electrons separated from the δ function by an energy equal to the

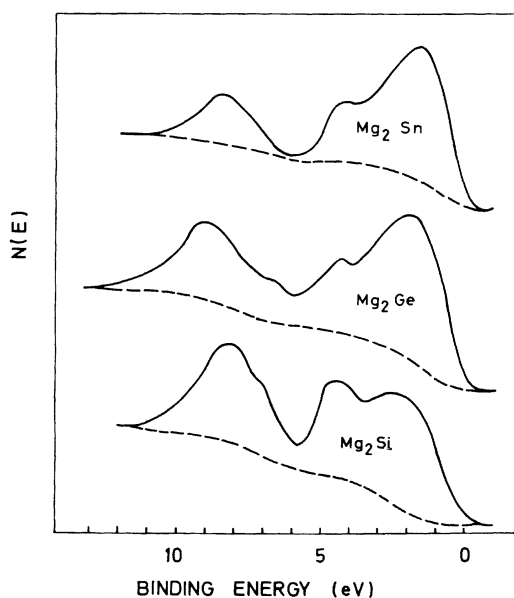


FIG. 2. Energy distribution spectra of photoelectrons excited with monochromatized Al $K\alpha$ radiation from the valence bands of Mg_2X compounds. The dashed line indicates the secondary electron contribution determined as discussed in Sec. III.

energy gap. The core-level spectra justify this approximation in the energy range of interest. For our purposes we can neglect the energy separation (~ 0.7 eV); our approximation becomes then that at any one energy the number of secondary electrons is proportional to the number of *primary* electrons at higher energies. This requires an iterative process. We therefore start from the crude estimate that the secondary contribution is simply a straight line from the top of the valence band to where the experimental curve levels off. These primary electrons are then used to obtain the second-order approximation with the above assumptions. The procedure converges rapidly. The corresponding estimates of the secondary electron emission are shown as dashed lines in Fig. 2.

The calculated band structure (Sec. II) shows that the valence bands can be divided into two groups: the upper three bands, with binding energies between 0 and 6 eV and the lower nearly s -like band, with binding energies between 6 and 10 eV. The upper three bands contain six electrons per primitive cell and can be subdivided into two groups: an upper set of two nearly degenerate p -like bands and a lower p - s hybridized band. In the XPS spectra of Mg_2Ge and Mg_2Sn the ratio of the areas of the peaks due to the upper bands to that due to the lower bands is indeed 3 : 1. Hence the ratio of p to s photoionization cross sections $\sigma_p/\sigma_s \approx 1$. For Mg_2Si , however, the ratio of those areas is considerably less than 3 : 1 thus indicating that $\sigma_p/\sigma_s < 1$. Similar results have been reported by Ley *et al.*³⁵ when comparing the XPS spectra of Si and Ge. This suggests once more that the electrons of Mg contribute little to the valence bands of Mg_2X , a fact which will be discussed again in Sec. IV.

IV. DISCUSSION

The EPM, as exemplified by AC's calculations (Sec. II), has been successfully used to obtain a complete picture of the energy bands of many semiconductors. This method obviates the difficulties of including the strongly divergent atomic potentials and the associated core levels in the calculation. Since the few required pseudopotential form factors can be treated as adjustable parameters, very good agreement with experiment can usually be obtained.

More recently, it has been shown by a number of workers that the valence band of tetrahedrally bonded semiconductors can be equally well described by a simple tight-binding model with a relatively small number of matrix elements treated as adjustable parameters. This model has the advantage of reducing the size of the secular ma-

trix and giving, in most cases, analytical expressions for the bands along high symmetry directions.³² It can be easily extended to include the atomic d levels present in alkali metal halides,³⁶ which are very difficult to treat within the pseudo-potential formalism.

Pantelides has also obtained valence bands for a large number of compounds with rock salt structure using the empirical tight-binding method (ETBM). He notes that, since the EPM has a free-electron starting point and the ETBM a free-atom starting point, the latter should be particularly suited for the usually more ionic crystals of the rocksalt structure. As discussed in Sec. I, it is impossible to construct a simple system of covalent bonds for the antifluorite structure. Based on the charge distribution experimentally obtained for Mg_2Si (see Sec. I) we are inclined to treat the Mg_2X structure as purely ionic, with all the s electrons of Mg transferred to the X atom. Under those conditions the ETBM band structure of these compounds is formally equivalent to that of a fcc Bravais lattice containing only the $2s$ and $6p$ electrons on the X atom (although the Mg atom can contribute to the potential). It is also equivalent to the ETBM band structure of a completely ionic rocksalt crystal calculated by Pantelides.³¹ We can thus use the parametrized secular matrix given by Pantelides for rocksalt to calculate the valence band of the Mg_2X compounds. It should be noted that in the matrix elements Pantelides measures k in units of $2/a$, one-half of the units used for zinc blende, and the different matrix elements are defined so as to be all positive. We shall use definitions similar to those given for zinc blende in Ref. 30.

We show in Fig. 1 our fit (solid line) to the AC calculations for Mg_2Si (dashed line); the corresponding interaction parameters are given in Table I, and the s - p splitting (Γ_{15} - Γ_1 splitting at $k=0$) in Table II. It can be seen that our bands can be made to reproduce closely those of the EPM in most symmetry directions: For practical purposes they may be considered equivalent. We can now obtain the corresponding DOVS, which we shall refer to as AC's. The integration method used is that of Gilat and Raubenheimer³⁷ with a mesh consisting of 916 points in the reduced Brillouin zone ($\frac{1}{48}$ of the full BZ). The DOVS so obtained is compared with our photoemission results for Mg_2Si in Fig. 3. We see that the agreement of the upper two peaks is satisfactory, but we do not find in photoemission the large gap between the upper and lower valence-band regions. With our resolution we should be able to see the asymmetric shape of the s level. The depth of the gap does depend somewhat on the correction for sec-

TABLE I. Parameters of the ETBM and BOM for the Mg_2X compounds and for the corresponding elements. $(X-X)$ represents the distance between nearest ($n=1$) and second nearest ($n=2$) X atoms, $(X-X)_n/(Si-Si)$ is this distance normalized by the nearest-neighbor distance of elemental Si. Unless otherwise indicated the parameters correspond to $n=1$.

	Mg ₂ Si AC ^a	Mg ₂ Si This work		Si Pandey and Phillips ^b		Si Harrison ^c		Mg ₂ Ge This work		Ge Pandey and Phillips ^b		Ge Harrison ^c		Mg ₂ Sn This work		Sn Harrison ^c	
		$n=1$	$n=2$	$n=1$	$n=2$	A	B	$n=1$	$n=2$	A	B	A	B	A	B	A	B
$(X-X)_n$	4.48	2.35	3.83	2.35	3.83	2.35	2.35	4.52	2.44	4.00	2.44	2.44	2.44	4.78	2.85		
$(X-X)_n$ (Si-Si)	1.90	1	1.63	1	1.63	1	1	1.9	1.04	1.70	1.04	1.04	1.04	2.03	1.21		
$(ss)_n$	-0.105	-2.08		-2.08		-1.38	-1.59	-0.250	-1.69		-1.23	-1.35	-1.23	-0.210	-0.98	-0.98	-0.99
$(sp)_n$	0	-2.12		-2.12		-1.94	-2.29	-0.7	-2.03	-2.19	-2.03	-2.19	-2.03	-0.550	-1.62	-1.62	-1.64
$(pp\sigma)_n$	-0.58	-2.32	-0.58	-2.32	-0.58	-0.23	-0.83	-0.84	-2.55	-0.11	-0.20	-0.61	-0.20	-0.72	-0.14	-0.14	-0.17
$(pp\pi)_n$	-0.02	-0.52	-0.10	-0.52	-0.10	-0.62	-0.62	-0.105	-0.67	-0.08	-0.68	-0.68	-0.68	-0.09	-0.55	-0.55	-0.55
V_1	0.11	0.04		0.552		0.85	0.85	0.05	0.37		0.82	0.82	0.82	0.03	0.68	0.68	0.68
V_2	1.86	1.25		4.095		2.2	3.0	1.29	4.095		2.15	2.7	2.15	1.06	1.76	1.80	1.80
V_4	0.06	-0.124		-0.245		-0.61	-0.61	-0.139	-0.398		-0.70	-0.70	-0.70	0.106	-0.58	-0.58	-0.58
V_5	0.04	-0.019		+0.275		0.01	0.01	-0.034	+0.272		-0.02	-0.02	-0.02	0.016	-0.03	-0.03	-0.03

^a From Ref. 20 (our fit).

^b From Ref. 39.

^c From Refs. 29(A) and 30(B).

TABLE II. Splitting of the $\Gamma_{15}-\Gamma_1$ valence states in Mg_2X compared with the corresponding $p-s$ splitting of the X atoms (nonrelativistic and relativistic calculations) and the $\Gamma_{25'}-\Gamma_{2'}$ splitting of the corresponding elemental semiconductor.

	Mg_2Si	Mg_2Ge	Mg_2Sn
This work	9.0	10	9.7
Au-Yang-Cohen ^a	9	9.9	8.7
Aymerich-Mula ^b	9	9.8	8.5
Folland ^c	8.9		
Lee ^d	9.0	9.3	
	Si	Ge	Sn
Free atom (nonrel.) ^e	7.0	8.0	6.55
Free atom (rel.) ^e	7.12	8.6	7.8
Elemental X crystal ^f	12.0	12.0	

^a From Ref. 20.

^b From Ref. 21.

^c From Ref. 19.

^d From Ref. 18.

^e From Ref. 23.

^f From Refs. 44 and 45.

ondary electrons, but no reasonable correction would give us anything close to the calculated gap.

A more striking failure of the AC results is observed when we consider the partial DOVS. Our fit of the AC's structure required no $s-p$ interaction [$(sp)=0$, see Table I] and therefore all the s electrons are contained in the narrow lower peak. Harrison's SXS results³⁸ (Fig. 4 solid line) show the L_{23} emission spectrum of Si in Mg_2Si (the upper scale refers to the energy of the emitted photons). This should give a convolution of the $L_{II,III}$ ($2p_{1/2,3/2}$) level shape with the s -like partial DOVS. In spite of the poor resolution it can be

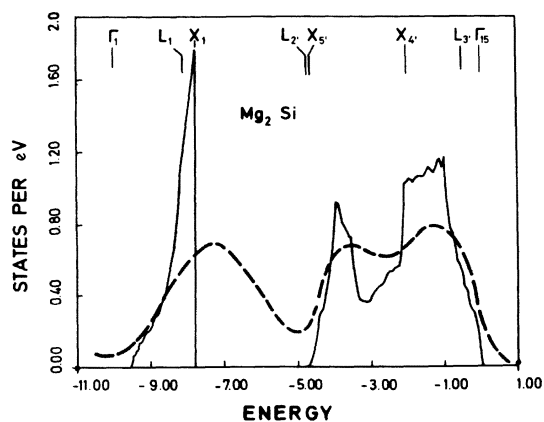


FIG. 3. Density of valence states calculated for the AC band structure of Mg_2Si (solid line) compared with the corresponding XPS spectrum after subtracting the secondary electrons contribution (dashed line).

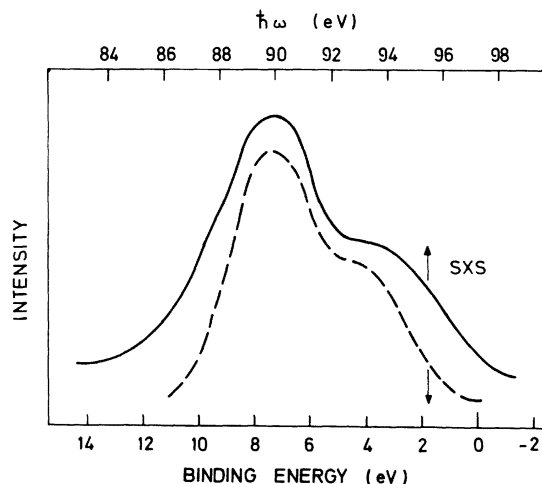


FIG. 4. Soft-X-ray emission (SXS) spectrum of Mg_2Si as obtained by Harrison (Ref. 38 solid line) compared with the partial- s density of states from the ETBM band structure, after convolution with a 2.5-eV FWHM Gaussian (dashed line). The calculated partial density of states has been shifted horizontally so as to align its main features with those of the experimental curve.

seen that the s -like electrons extend into the upper, mostly p region; thus the $s-p$ interaction cannot be neglected.

The photoemission results for Mg_2Ge indicate a similar DOVS to that of Mg_2Si . Again, the separation between upper and lower regions is not as marked as expected from AC calculations (we do not show AC's DOVS for Mg_2Ge or Mg_2Sn , but it can be seen that they are basically the same as for Mg_2Si). Only for Mg_2Sn do we find a clear gap, nevertheless even here the lower region is more symmetric than that obtained from AC's bands. Unfortunately no SXS measurements are available for these materials. The fact that the ϵ_2 experimental curves agree well with AC's results means that the upper valence bands, which are those probed in the optical measurements, are probably correct, while XPS and SXS indicate that the lower levels are not correct. This is not surprising in view of the fact that the lower bands do not contribute to ϵ_2 at low energies, which was used for adjusting AC's parameters.

We shall proceed now to use the ETBM to obtain band structures of Mg_2X subjected to the following constraints: (i) The upper bands should be similar to those of AC; (ii) the calculated DOVS should correspond to the XPS results; (iii) for Mg_2Si , the partial s DOVS should reproduce the SXS results once the appropriate broadening is included; (iv) since no equivalent SXS results are available for Mg_2Ge and Mg_2Sn , the ETBM parameters for these materials should be related to those of Mg_2Si and

the crystal parameters in a simple, reasonable way.

In order to obtain the correct partial s DOVS a large (sp) term is needed. This introduces a large repulsion between the lower p and s bands, and requires a readjustment of all the parameters. The resulting band structure is shown by the solid lines in Fig. 5, compared with AC's band structure (dashed curve). Since our upper valence bands are not greatly distorted when compared with AC's, a mixed basis ϵ_2 calculation using AC's (or Aymerich and Mula's) conduction bands and our valence bands should give similar low-energy critical points as those obtained by AC. However, the s - p mixing on the lower valence bands should decrease the transition probability to the lower conduction bands (s or d symmetry) in the 4–8-eV range. The corresponding reduction in the intensity of the spectrum may produce better agreement with experiment. However, a detailed calculation of ϵ_2 would take us beyond the scope of the present work.

The corresponding total and s -partial DOVS without any smoothing are shown in Fig. 6. Some of the symmetry points are indicated. The dashed curve represents the XPS results. The agreement between XPS results and the total DOVS is good, especially when we allow for the smaller weight of the p with respect to the s cross section. The calculated partial- s DOVS, convoluted with a 2.5 eV full width at half maximum (FWHM) Gaussian was plotted as a dashed line in Fig. 4. It was positioned to correspond to the SXS results. The lower-energy scale gives the binding energy with respect to the top of the valence band. Comparing the two curves of Fig. 4 one obtains that the energy of the center of mass of the $L_{2,3}$ levels measured with respect to the top of the

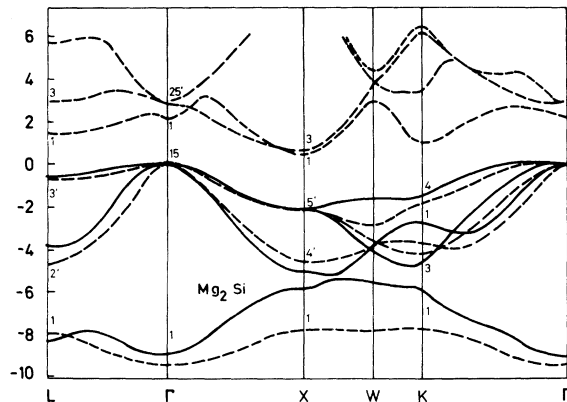


FIG. 5. Band structure of Mg_2Si as obtained with the ETBM (solid line), compared with AC's calculations performed with the EPM (dashed line). The energy is given in eV.

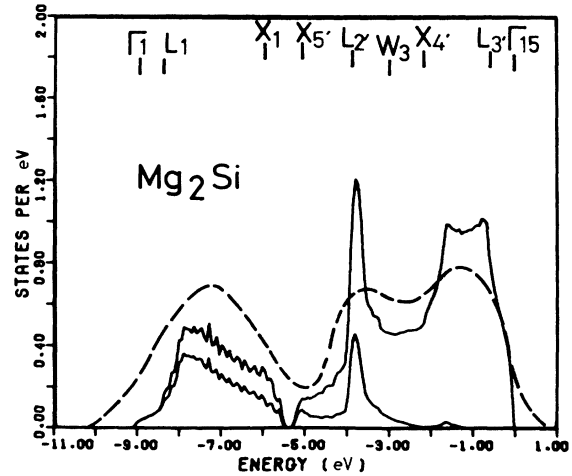


FIG. 6. Total and partial s density of valence states calculated for the ETBM band structure of Mg_2Si (solid line) compared with the corresponding XPS spectra after subtracting the secondary electron contribution (dashed line). The position of some high-symmetry points is indicated.

valence band is 97.4 eV, in reasonable agreement with the value from the XPS core levels reported in I (98.4 ± 0.2 eV) measured with respect to the Fermi level.

The band structure and the total and partial- s DOVS of Mg_2Ge are shown in Figs. 7 (solid line) and 8, respectively. The position of the s level (E_s) had to be increased to obtain the best fit to experiment. This required an increase of the (sp) matrix element to maintain the required repulsion and the position of the lower p band. Since the lattice parameter of Mg_2Ge is practically the same as that of Mg_2Si , this does not seem to fulfill point (iv) above. In spite of it we see that, as

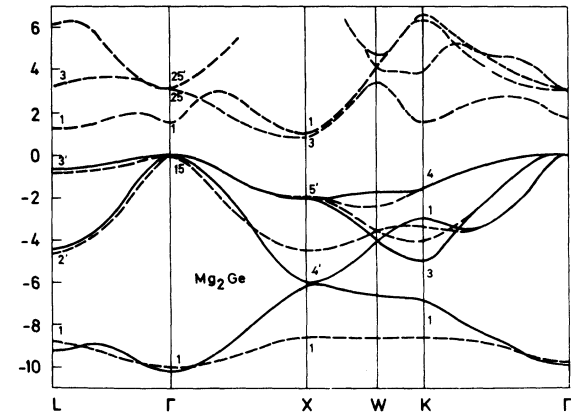


FIG. 7. Band structure of Mg_2Ge as obtained with the ETBM (solid line), compared with AC's calculations performed with the EPM (dashed line). The energy is given in eV.

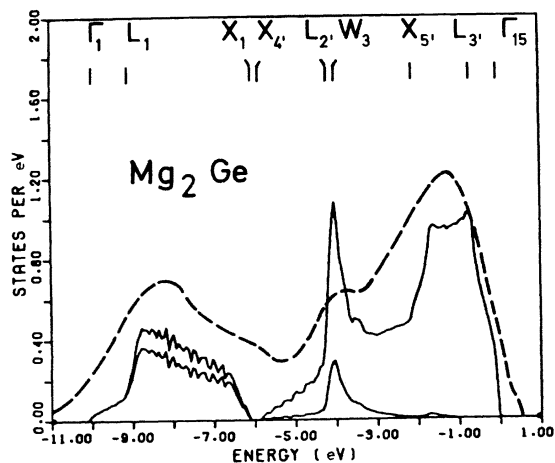


FIG. 8. Total and partial s density of valence states calculated for the ETBM band structure of Mg_2Ge (solid line) compared with the corresponding XPS spectra after subtracting the secondary electron contribution (dashed line). The position of some high-symmetry points is indicated.

in Mg_2Si , we do obtain a nearly zero gap between the upper and lower regions (the small gap that seems to appear in Fig. 8 (0.3 eV) is an artifact of the integration procedure; a zero gap follows from the solid lines of Fig. 7). The interaction parameters for Mg_2Sn (see Figs. 9 and 10) are obtained from those of Mg_2Si when a scaling like $1/a^2$ is included (a is the lattice parameter); E_s is fixed independently. We see that a clear gap develops, in agreement with the photoemission results.

The LCAO parameters (nm) used in previous band structures are given in Table I, along with the corresponding parameters (V_m) of the bond-

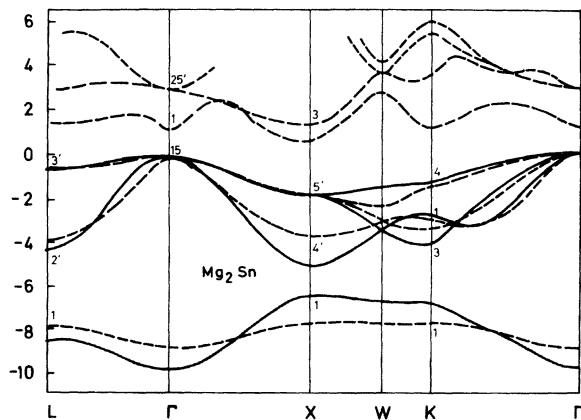


FIG. 9. Band structure of Mg_2Sn as obtained with the ETBM (solid line), compared with AC's calculations performed with the EPM (dashed line). The energy is given in eV.

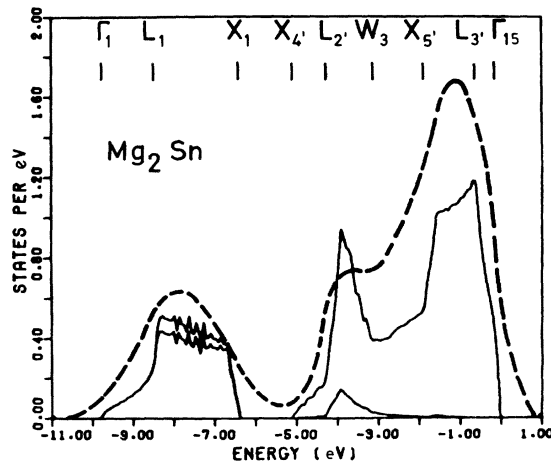


FIG. 10. Total and partial s density of valence states calculated for the ETBM band structure of Mg_2Sn (solid line) compared with the corresponding XPS spectra after subtracting the secondary electron contribution (dashed line). The position of some high-symmetry points is indicated.

orbital model (BOM). The V_m 's are defined as interactions between sp^3 hybridized orbitals and the (nm) as those between atomic levels. The two basis sets are equivalent for tight-binding calculations; the transformation from one set to the other can be easily performed with the expression of Ref. 30. We also include both representations for the parameters used by Pandey and Phillips³⁹ (basically LCAO) and Harrison and coworkers (basically BOM). Pandey and Phillips used both nearest- and next-nearest-neighbor interactions and we shall refer to the second ones as (nm)₂, as customary. In Ref. 30, Pantelides and Harrison do not give V_2 explicitly since it enters the band calculation together with another parameter (V_3) and only their ratio is important and thus we have taken V_2 from Refs. 29 (A) and 30 (B). These authors do not treat V_2 as a free parameter: it is obtained from the dielectric constant.

We can expect ($pp\sigma$) to be larger than ($pp\pi$), that is, the interaction between two p orbitals pointing along the same bond should be larger than between different parallel bonds; this is the case in our calculations as well as Pandey and Phillips's [this in fact holds even for (pp)₂] and Harrison's (B), but ($pp\sigma$) is small when compared with (sp) or Pandey and Phillips's. This is caused by the small value of V_2 . In Harrison's (A) ($pp\sigma$) is smaller than ($pp\pi$). Also in all cases, (sp) is larger than (ss). All our parameters are smaller than the corresponding ones for elemental Si or Ge, but trying to obtain the former from the latter by means of a simple square or cubic dependence on the interatomic distance can only be a crude

approximation.

(It should be remembered that atomic functions centered on different atoms are not orthogonal, and orthogonalized Löwdin functions⁴⁰ should be used to define and calculate these interactions. These functions have the same symmetry properties as the original ones, but have a larger spatial extent⁴¹.)

We find that for our ETBM band structures of Mg_2X ($pp\sigma$)/($pp\pi$) = 8: the same ratio was found by Pantelides for rocksalt materials.³¹ We may therefore conclude that this ratio is a consequence of the crystal structure.

We give in Table II the s - p splittings (identical to the Γ_1 - Γ_{15} splitting at $k=0$) in the Mg_2X compounds resulting from different calculations, as well as those for the free atom and for the elemental crystals. First we note that in the non-relativistic free-atomic calculation,²² the splitting in Sn is the smallest whereas in the relativistic one it lies between those of Si and Ge. Our results scale with the relativistic results for the free atom, which is not surprising since our values are obtained from a fit to experimental XPS data. The splitting of other nonrelativistic band calculations resembles the nonrelativistic free atom, as expected. In the pure Si and Ge crystals the splitting is strongly affected by the large interaction^{30,32} and is therefore not so simply related

to the atomic values. In the rocksalt (Mg_2X) case it is mainly determined by the unperturbed energies of the atomic s and p states.

We mentioned in paper I that the fact that the spin-orbit splitting Δ_0 in Mg_2Ge (0.2 eV) was smaller than in the crystal (0.3 eV) had been explained as due to a $\frac{2}{3}$ - $\frac{1}{3}$ sharing of the valence electrons between the Ge and Mg atoms. Nevertheless, since the spin-orbit splitting of the $4p$ electrons of atomic Ge is also 0.2 eV,²³ the splitting in Mg_2Ge could simply be due to the larger Ge-Ge separation, 1.85 times that in the Ge crystal. We note that Δ_0 increases with decreasing lattice constant.⁴² It is also interesting to point out that for outermost d levels of a number of elements larger spin-orbit splittings are found in the condensed elemental form than in either the free atom, compounds, or diluted alloy.⁴⁴ Finally we would like to mention that the transfer of charge from the Mg to the anion implicit in our model and in Ref. 13 is supported by the core shifts reported in I.

ACKNOWLEDGMENTS

We would like to express our thanks to H. Schwarz and W. Hägele for their help in running the computer programs used for the calculations, and Dr. E. Schönherr for providing us with the sputtering targets.

¹A. L. Norbury, Proc. Faraday Soc. **16**, 570 (1921).

²G. Busch and U. Winkler, Helv. Phys. Acta **26**, 579 (1953); Physica (Utr.) **20**, 1067 (1954); U. Winkler, Helv. Phys. Acta **28**, 635 (1955).

³W. D. Robertson and H. H. Uhlig, Trans. Metall. Soc. AIME **96**, 27 (1949).

⁴G. A. Stringer and R. J. Higgins, J. Appl. Phys. **41**, 489 (1970).

⁵N. F. Mott and H. Jones, *The Theory of Metals and Alloys* (Dover, New York, 1954).

⁶R. J. Kearney, T. G. Worlton, and R. E. Schmunk, J. Phys. Chem. Solids **31**, 1085 (1970).

⁷W. B. Whitten, P. L. Chung, and G. C. Danielson, J. Phys. Chem. Solids **26**, 49 (1965).

⁸P. L. Chung, W. B. Whitten, and G. C. Danielson, J. Phys. Chem. Solids **26**, 1753 (1965).

⁹S. Onari, E. Anastassakis, and M. Cardona, in *Light Scattering in Solids*, edited by M. Balsamski, R. C. C. Leile, and S. P. S. Porto, (Flammarion, Paris, 1976), p. 54.

¹⁰D. McWilliams and D. W. Lynch, Phys. Rev. **130**, 2248 (1963).

¹¹J. M. Eldridge, E. Miller, and K. L. Komarek, Trans. Metall. Soc. AIME **239**, 775 (1967).

¹²N. V. Ageev and L. N. Guseva, Bull. Acad. Sci. USSR Div. Chem. Sci. **1**, 31 (1952) (quoted extensively by N. Folland in Ref. 19).

¹³D. Pankel and E. Woelfel, Z. Kristallogr. **129**, 9 (1969).

¹⁴A. Stella and D. W. Lynch, J. Phys. Chem. Solids **25**, 1253 (1964), and references therein.

¹⁵W. J. Scouler, Phys. Rev. **178**, 1353 (1969).

¹⁶F. Vazquez, R. A. Forman, and M. Cardona, Phys. Rev. **176**, 905 (1968).

¹⁷J. Della Riccia, in *Proceedings of the International Conference on Semiconductor Physics*, Prague, 1960 (Academic, New York, 1961), p. 51.

¹⁸P. M. Lee, Phys. Rev. **135**, A1110 (1964).

¹⁹N. O. Folland, Phys. Rev. **158**, 764 (1967).

²⁰M. Y. Au-Yang and M. Cohen Solid State Commun. **6**, 855 (1968); and Phys. Rev. **141**, 789 (1966).

²¹F. Aymerich and G. Mula, Phys. Status Solidi B **42**, 697 (1970).

²² Mg_2Si : W. B. Whitten and G. C. Danielson, in *Proceedings of the Seventh International Conference in the Physics of Semiconductors*, Paris (Dunod, Paris, 1964), p. 537 (Piezoresistance); Mg_2Sn : J. Umeda, J. Phys. Soc. Jpn. **18**, 2052 (1969) (magnetoresistance); Mg_2Ge : P. W. Li, S. N. Lee, and G. C. Danielson, Phys. Rev. B **6**, 442 (1972) (magnetoresistance).

²³F. Herman and S. Skillman, *Atomic Structure Calculations* (Prentice-Hall, Englewood Cliffs, N. J., 1963).

²⁴J. Tejada, M. Cardona, N. J. Shevchik, D. W. Langer, and E. Schönherr, Phys. Status Solidi B **58**, 189 (1973).

²⁵M. Cardona, J. Tejada, N. J. Shevchik, and D. W. Langer, Phys. Status Solidi B **58**, 483 (1973).

²⁶G. G. Hall, Philos. Mag. **43**, 338 (1953); **3**, 429 (1958).

- ²⁷D. Stocker, Proc. R. Soc. A 270, 397 (1962).
- ²⁸G. Leman and Friedel, J. Appl. Phys. Suppl. 33, 281 (1962).
- ²⁹W. A. Harrison, Phys. Rev. B 6, 4487 (1973); and W. A. Harrison and S. Ciraci, *ibid.* 10, 1516 (1974).
- ³⁰S. T. Pantelides and W. A. Harrison, Phys. Rev. B 11, 3006 (1975).
- ³¹S. T. Pantelides, Phys. Rev. B 11, 5082 (1975).
- ³²N. J. Shevchik, J. Tejada, and M. Cardona, Phys. Rev. B 9, 2627 (1974).
- ³³H. Krebs and W. Schottky, *Halbeiterprobleme I* (Kieweg, Braunschweig, 1954), p. 42.
- ³⁴N. O. Folland and F. Bassani, J. Phys. Chem. Solids 29, 281 (1968).
- ³⁵L. Ley, S. Kowalczyk, R. Pollak, and D. A. Shirley, Phys. Rev. Lett. 29, 1088 (1972).
- ³⁶J. Tejada, N. J. Shevchik, W. Braun, A. Goldmann, and M. Cardona, Phys. Rev. B 12, 1557 (1975).
- ³⁷G. Gilat and L. J. Raubenheimer, Phys. Rev. 144, 390 (1966).
- ³⁸R. Harrison, Philos. Mag. 22, (175), 131 (1970).
- ³⁹K. C. Pandey and J. C. Phillips, Phys. Rev. 13, 750 (1976).
- ⁴⁰P. O. Löwdin, J. Chem. Phys. 18, 365 (1950).
- ⁴¹J. C. Slater and G. F. Koster, Phys. Rev. 94, 1498 (1954).
- ⁴²F. Cerdeira, J. Dewitt, U. Rössler, and M. Cardona, Phys. Status Solidi B 41, 735 (1970).
- ⁴³N. J. Shevchik, J. Tejada, M. Cardona, and D. W. Langner, Phys. Status Solidi B 59, 87 (1973).
- ⁴⁴L. Ley, R. A. Pollak, F. R. McFeely, S. P. Kowalczyk, and D. A. Shirley, Phys. Rev. 9, 600 (1974).
- ⁴⁵D. J. Stukel, T. C. Collins, and R. W. Euwema, in *Electronic Density of States*, Nat. Bur. Stds. Special Pub. No. 323 (U. S. GPO, Washington, D. C. 1971), p. 93.